LANGMUIR

pubs.acs.org/Langmuir Article

Interactions of the Cocaine and Quinine Aptamer with Gold Nanoparticles under the Dilute Biosensor and Concentrated NMR Conditions

Fang Zhang and Juewen Liu*

Cite This: *Langmuir* 2021, 37, 11939−11947

Read Online

ACCESS | Metrics & More | Article Recommendations

ABSTRACT: The cocaine aptamer was later found to bind quinine with an even higher affinity. In this work, we used a fluorescently labeled aptamer named MN4 to study its adsorption by gold nanoparticles (AuNPs), and the subsequent displacement by the nonlabeled aptamer and by quinine. Without washing, 14% of the preadsorbed MN4 strands were displaced by 4000-fold excess of free MN4, whereas no displacement was observed after washing, suggesting that washing removed weakly adsorbed aptamers. In a previous paper, rapid exchange was observed with NMR by directly mixing AuNPs and concentrated MN4, and our work has unified the dilute and concentrated aptamer conditions. The difference is attributable to the conformation of the adsorbed aptamer, where dilute aptamers are adsorbed in a collapsed state with a much higher affinity to AuNPs. In addition, the preadsorbed MN4 aptamer cannot be desorbed by adding quinine, indicating that direct desorption-based fluorescent sensors cannot be made. Finally, based on the similar color responses to both the aptamer and its nonbinding mutants, the label-free colorimetric detection method cannot be directly applied for the detection of quinine. This work indicated that different experimental conditions need to be carefully compared to have a unified understanding of aptamer/AuNP systems.

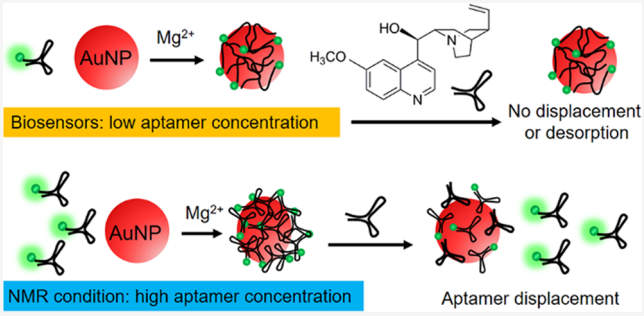

INTRODUCTION

DNA probes and gold nanoparticles (AuNPs) have been used in the development of optical biosensors for a long time.[1−8] AuNPs are excellent fluorescence quenchers with extremely high extinction coefficients,[9,10] and they can also strongly adsorb DNA oligonucleotides.[11,12] We demonstrated that adsorbed 15-mer DNA cannot be desorbed by adding its complementary DNA (cDNA), supporting the strong adsorption affinity.[13] In addition, we studied a few DNA aptamers (e.g., for adenosine, lysozyme, and Hg^{2+}) and concluded that none of them could be desorbed from AuNPs by adding their target molecules.[13]

Similar observations were also observed on planar gold surfaces,[14] although very short DNA oligoes, such as 5-mer, were reported to experience DNA-induced displacement, especially with a very high concentration of salt (e.g., 1 M NaCl).[15] However, most DNA probes and aptamers are much longer than 5-mer,[16,17] and AuNPs can hardly survive such high ionic strength. In addition, since each DNA sequence is different, they may have distinct secondary and tertiary structures. When a well-folded DNA is adsorbed, it could be that only a few bases contact AuNPs, leading to a lower adsorption affinity. However, few studies touched upon the conformation of adsorbed DNA on AuNPs.

The cocaine aptamer has been extensively studied,[18] including its truncation, splitting, and mutation,[19−23] and use for the detection of cocaine.[24−27] Its adsorption on AuNPs was recently studied by NMR spectroscopy, and the rapid exchange of the adsorbed and nonadsorbed aptamers was observed at the NMR time scale.[28] However, the experimental condition of NMR is very different from typical conditions used for biosensors. For example, the concentration of DNA was very high for NMR, while the concentration of the AuNPs was much lower (DNA/AuNP = 10000:1). The high DNA concentration might allow a crowded packing of DNA, and thus, the likelihood of DNA collapsing on AuNPs decreased. For a biosensor work, a washing step is often performed to remove nonadsorbed or weakly adsorbed DNA, or a very low DNA concentration was used to ensure a low background (e.g., DNA/AuNP < 100:1).[29−31] For a 13 nm AuNP, its adsorption capacity is typically below 100 nonthiolated DNA strands.[32]

Received: August 21, 2021
Revised: September 11, 2021
Published: September 30, 2021

https://doi.org/10.1021/acs.langmuir.1c02239
Langmuir 2021, 37, 11939−11947

The high fraction of free DNA (e.g., >99%) in the NMR condition may also promote displacement or exchange with the adsorbed DNA.

To understand the concentration gap between the NMR and biosensor conditions and unify the observations at both high and low concentrations of DNA, we herein studied the cocaine aptamer as a model system. Since this aptamer can actually bind quinine much better,[33,34] we used quinine instead of cocaine as the target molecule. The aptamer and AuNPs have been interfaced to detect cocaine,[26,28,35] but the understanding of quinine is limited. Furthermore, in this study, adsorption of quinine on AuNPs, its effect on the adsorption of the aptamer, and potential fluorescent and colorimetric detection were also studied, which are critical for designing related biosensors.[36−42] Our results indicated that not only DNA sequence and structure but also DNA concentration, washing, and incubation time are critical. This work also points out that different experimental conditions in different spectroscopic techniques need to be considered to unify our understanding.

MATERIALS AND METHODS

Chemicals. The DNA samples used in this work were all purchased from Integrated DNA Technologies (Coralville, IA) and listed in Table 1. Trisodium citrate dihydrate, sodium phosphate monobasic monohydrate, sodium phosphate dibasic heptahydrate, adenosine, and sodium fluoride (NaF) were obtained from Mandel Scientific (Guelph, ON, Canada). Potassium cyanide (KCN) and quinine hemisulfate monohydrate were from Sigma-Aldrich. Thiolated methoxypolyethylene glycol (SH-PEG, molecular weight: 1 K) was from Nanocs (New York, NY). Citrate-capped AuNPs (13 nm) were synthesized according to the literature using citrate reduction, and the as-synthesized AuNPs were ∼10 nM.[43] Milli-Q water was used for preparing all of the buffers and solutions.

Table 1. DNA Sequences Used in This Work[a]

names	sequences and modifications (5′−3′)
FAM-MN4	GGCGACAAGGAAAATCCTTCAACGAAGTGGGTCGCC-FAM
FAM-Ade	FAM-ACCTGGGGGAGTATTGCGGAGGAAGGT
FAM-T_5	FAM-TTTTT
FAM-A_5	FAM-AAAAA
A_{15}	AAAAAAAAAAAAAAA
Ade aptamer	ACCTGGGGGAGTATTGCGGAGGAAGGT
MN4	GGCGACAAGGAAAATCCTTCAACGAAGTGGGTCGCC
MN2	GGCGACAAGGAAAATCCTTCAAAAGGGTCGAC
MN12	GGCGACCAGGAAAATCCTTCAACGAAGTGGGTCGCC
MN16	GGCGACAAGGAAAATCCTACAACGAAGTGGGTCGCC

[a]FAM: carboxyfluorescein.

Preparation of FAM-DNA-Adsorbed AuNPs. FAM-DNA/AuNP conjugates were prepared by adding 3 μL of FAM-DNA (100 μM) into 150 μL of AuNPs (10 nM) and incubated at room temperature for 3−4 h. After that, 150 μL of phosphate buffer (PB, 20 mM, pH 7.6) containing 2 mM $MgCl_2$ was added and the sample was stored at 4 °C overnight. Then, the free nonadsorbed FAM-DNA strands were removed by centrifugation at 14 000 rpm for 10 min and washed with 10 mM PB (pH 7.6) 3−4 times until the supernatant had no fluorescence under a UV lamp. Finally, the precipitate was resuspended in 50 μL of 10 mM PB (pH 7.6). The concentration of the AuNPs was calculated based on the extinction coefficient (2.7×10^8 M^{-1} cm^{-1}) at 520 nm.

DNA Desorption Kinetics (with Washing). To study DNA desorption, the FAM-DNA/AuNP conjugates prepared above were exposed to either a high concentration of nonlabeled DNA or quinine, and the fluorescence increase was monitored. In a typical experiment, the fluorescence of FAM-DNA/AuNP (0.7 nM AuNPs) in 10 mM PB (pH 7.6) with 0.8 mM $MgCl_2$ (total 96 μL) was first monitored for 3 min (Ex: 485 nm; Em: 535 nm). Then, 4 μL of 5 mM DNA (final 200 μM) or 1 mg/mL quinine (final ∼ 100 μM) in the same buffer was added into the cuvette, mixed, and monitored for another 20−30 min. After that, 1 μL of KCN (1 M) was added to dissolve the AuNPs and fully release the remaining FAM-DNA. The fluorescence data were then normalized to have the final fluorescence being 1.

Adsorption and Desorption Kinetics (without Washing). To study DNA desorption without washing away the nonadsorbed DNA, the FAM-DNA adsorption kinetics were first monitored in real time. For the MN4 aptamer, the fluorescence of 86 μL of the sample including 3 μL of FAM-MN4 (1 μM), 4.3 μL of PB (100 mM), and 8.6 μL of $MgCl_2$ (10 mM) was first monitored for 2 min as the initial fluorescence (F_0), where the final PB buffer concentration was 5 mM and $MgCl_2$ was 1 mM. Then, 10 μL of the AuNP sample (5 nM dispersed in 5 mM PB, pH 7.6) was added into the cuvette and the fluorescence was monitored for another 10 min. After that, 4 μL of MN4 (5 mM) dissolved in PB (10 mM, pH 7.6 with 0.8 mM $MgCl_2$) was added to desorb FAM-MN4 from the AuNPs. For the adenosine aptamer, 86 μL of the mixture included 1 μL of FAM-Ade (1 μM), 4.3 μL of PB (100 mM), and 4.3 μL of $MgCl_2$ (10 mM), where the final PB buffer concentration was 5 mM and $MgCl_2$ was 0.5 mM. After the addition of 10 μL of the AuNP sample (5 nM dispersed in 5 mM PB, pH 7.6), 4 μL of the 5 mM nonlabeled adenosine aptamer in PB (10 mM, pH 7.6 with 0.8 mM $MgCl_2$) was added. Here, the initial FAM-DNA concentration was different from the above washed samples since we optimized the conditions so that both washed and unwashed samples had a similar DNA adsorption density.

AuNP Stability. To study the effect of quine toward the colloidal stability of AuNPs in the absence of DNA, 1 μL of the quinine solution (5 μg/mL or 12.5 μM) was added into 100 μL of AuNPs (2 nM) each time and around 15 additions were made. The UV−vis absorption spectra were recorded with a microplate reader (Tecan Spark) and the extinction ratio of 618 nm over 520 nm was calculated. To study the effect of quine toward AuNP stability in the presence of DNA, 2 nM AuNPs in 5 mM PB were premixed with 120 nM DNA and then titrated by the quinine solution.

Colorimetric Sensing. To evaluate the colorimetric sensing performance with MN4 and AuNPs, two methods were used. The first one followed the procedure described in the NMR paper.[28] DNA/AuNP conjugates were prepared before adding quinine. DNA (100 μM, 6 μL) was mixed with 13 nm AuNPs (10 nM, 1 mL) and incubated at room temperature for 3−4 h. Then, 1 mL of PB (20 mM, pH 7.6, 2 mM $MgCl_2$) was added into the mixture and stored at 4 °C overnight. Without washing, 90 μL of the DNA/AuNP complex was separately mixed with 10 μL of quinine solutions of different concentrations. Afterward, 2.5 μL of NaCl (3 M) was added to induce the aggregation of the AuNPs. Two minutes later, the extinction ratio of 618 and 520 nm was recorded. The other colorimetric sensing procedure used was conducted by first mixing the aptamer DNA with quinine before adding AuNPs. The DNA-quinine solution (50 μL) was prepared by adding 3 μL of DNA (10 μM), 20 μL of PB (pH 7.6, 100 mM), 17 μL of H_2O, and 10 μL of the quinine solution. After incubation at room temperature for 15 min, 50 μL of AuNPs (10 nM) were added. Two minutes later, the extinction ratio of 618 and 520 nm was recorded.

RESULTS AND DISCUSSION

Cocaine (Quinine) Aptamer. The secondary structure of the aptamer named MN4 is shown in Figure 1A. It forms a stable three-way junction, and stem 1 is always closed regardless of the presence or absence of target molecules.[44] This aptamer can bind both cocaine and quinine, and the affinity for quinine is even higher. Therefore, we used quinine as the target in this work (Figure 1C). Besides MN4, a few nonbinding mutants, namely, MN2, MN12, and MN16, were

https://doi.org/10.1021/acs.langmuir.1c02239
Langmuir 2021, 37, 11939−11947

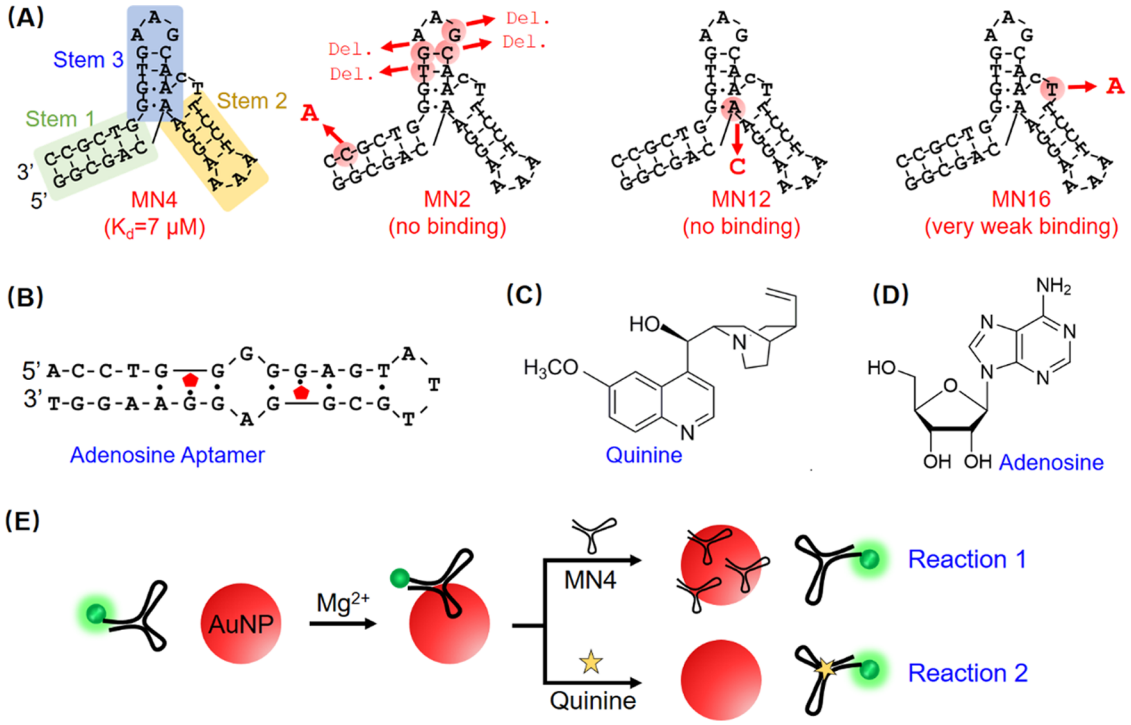

Figure 1. Structures of (A) the NM4 aptamer and a few nonbinding mutants and (C) its target quinine. The structures of (B) the adenosine aptamer and (D) its target adenosine. (E) A scheme showing the adsorption of FAM-labeled MN4 to AuNPs with fluorescence quenched, and the addition of nonlabeled MN4 for displacement (reaction 1) and its target to induce aptamer desorption (reaction 2) with an increase in the fluorescence.

tested as control sequences (Figure 1A). These controls had only one or a few base differences compared to MN4, and thus, the overall folded structure could be retained. To have a complete understanding, we also included the adenosine aptamer (Figure 1B; the structure of adenosine is shown in Figure 1D), A_{15}, as well as FAM-labeled A_5 and T_5 DNA.[45−47]

NMR showed that the MN4 aptamer used the tri-adenine loop in stem 2 to adsorb to AuNPs, and rapid exchange between the adsorbed and nonadsorbed aptamers was observed.[28] Upon the addition of the target molecule, the equilibrium was shifted to the desorbed state, and it was believed that target binding to the aptamer was the reason for this shift. However, the NMR experiment used a very large excess of the aptamer (200 μM) compared to the AuNPs (20 nM), which was far away from the aptamer concentration for most biosensor experiments (often in the low μM to low nM region). Therefore, we herein used a 3′-end carboxyfluorescein (FAM)-labeled MN4 aptamer to understand this concentration gap.

Fluorescence Spectroscopy for Studying Free Aptamer Adsorption. To evaluate the exchange between the adsorbed aptamers and free aptamers in a typical sensing condition, we first adsorbed FAM-MN4 onto 13 nm of AuNPs using the $MgCl_2$ aging method as described in the NMR paper.[28] The difference was that in the NMR experiment, no washing was performed, but we washed away the nonadsorbed FAM-MN4 with buffer after centrifugation. We then monitored the fluorescence increase indicative of FAM-MN4 desorption after adding a high concentration (200 μM) of nonlabeled MN4 (schematically shown in Figure 1E, reaction 1). We chose 200 μM MN4 since this was the concentration used in the NMR experiment. To minimize the inner filter effect (e.g., absorption of excitation and emitted light by the AuNPs), our final AuNP concentration was 0.7 nM, which was lower than 20 nM used for the NMR. Given the large excess of the free DNA, the difference in AuNP concentration would not significantly affect the displacement kinetics. We measured the adsorbed FAM-MN4 on these AuNPs to be 47.3 nM (MN4/AuNP = 68:1). Therefore, the ratio of the nonlabeled MN4 and the adsorbed FAM-MN4 was more than 4000:1. Given such a high ratio, we can assume that desorbed FAM-MN4 cannot be readsorbed, and desorption of FAM-MN4 would result in a fluorescence increase. At the end of the experiment, KCN was added to fully release all of the FAM-MN4 and the final fluorescence was used to calculate the percentage of the FAM-MN4 released in the previous step. As shown in Figure 2A, only ∼1% FAM-MN4 desorbed from the surface at 50 min after adding 200 μM MN4 DNA (inset). Almost the same amount of FAM-MN4 was desorbed when only buffer was added, indicating the observed 1% desorption was nonspecific instead of competition from free MN4.

In addition, we also studied the FAM-labeled adenosine aptamer (FAM-Ade) using the same method (Figure 2B). In this case, the adsorbed FAM-Ade probes were seldom desorbed by 200 μM nonlabeled aptamer either. Although compared to the NMR experiment, our DNA probe contained an extra FAM label, the FAM label did not contribute much to the adsorption, and the adsorption affinity was dominated by the DNA sequence. For example, FAM-labeled poly-A DNA was adsorbed much strongly than FAM-poly-T DNA.[32] Therefore, we concluded that no exchange of the adsorbed aptamer occurred in the traditional sensing procedure (e.g., a low initial aptamer probe concentration and free probes removed) even when a large excess of free aptamers were present, suggesting very stable aptamer adsorption by AuNPs.

https://doi.org/10.1021/acs.langmuir.1c02239
Langmuir 2021, 37, 11939−11947

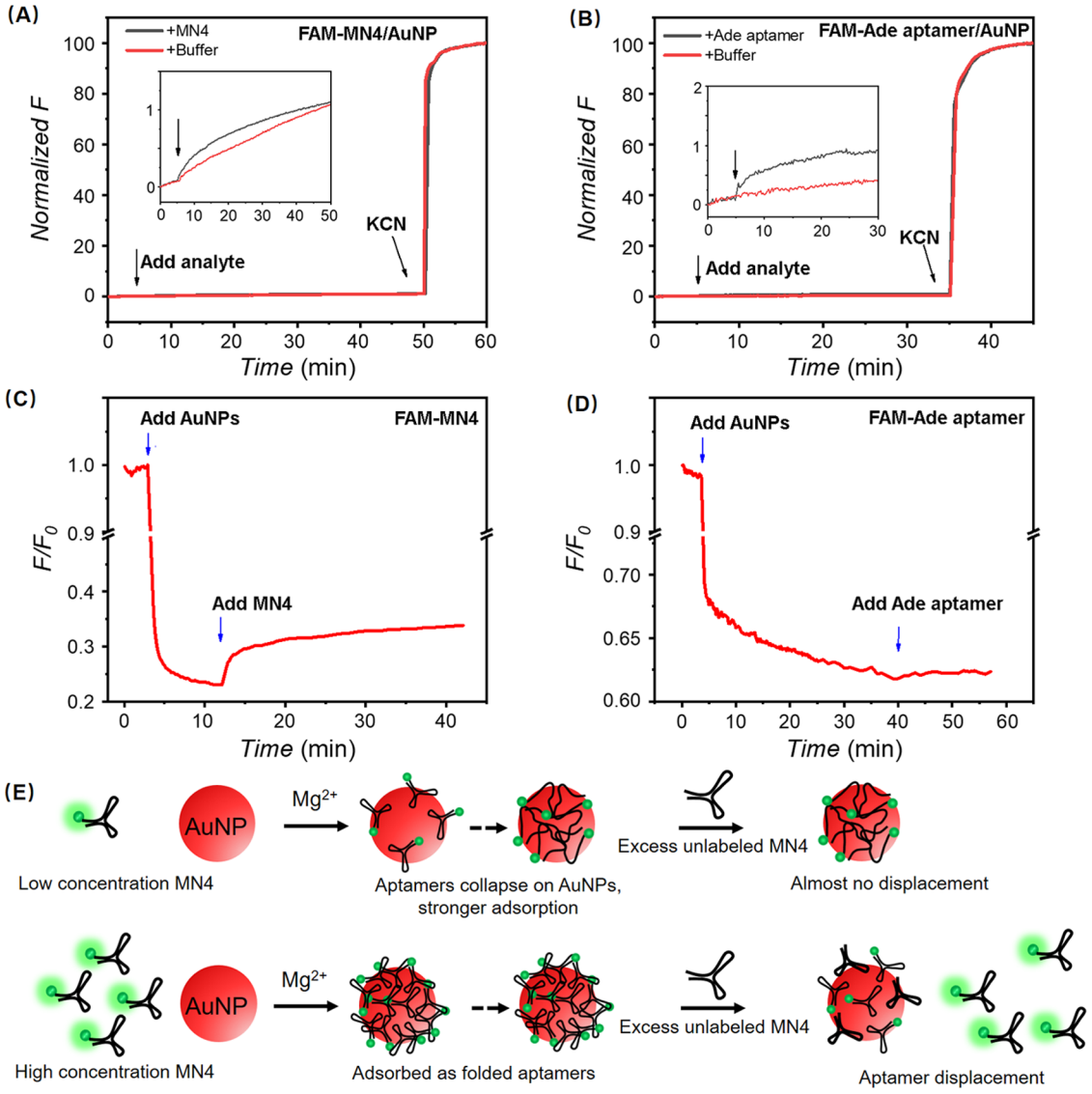

Figure 2. Desorption of (A) FAM-MN4 and (B) FAM-Ade by 200 μM nonlabeled MN4 or Ade aptamer from AuNPs prepared through the adsorption and washing steps. The buffer contained 10 mM PB and 0.8 mM $MgCl_2$. Insets: the same plot with a small *y*-axis scale. Kinetics of (C) FAM-MN4 and (D) FAM-Ade adsorption followed by desorption. FAM-labeled aptamers (30 nM) were first adsorbed onto 0.5 nM AuNPs and monitored for (C) 10 min for FAM-MN4 or (D) 40 min for FAM-Ade until the fluorescence stabilized. Then, 200 μM nonlabeled aptamer was added. (E) Scheme showing the stable adsorption of a low concentration of the collapsed MN4 aptamer that cannot be displaced, and the rapid exchange of the folded MN4 when adsorbed at a high concentration.

The strong DNA adsorption by AuNPs was consistent with the previous work.[13,14]

While our fluorescence experiment had the same total DNA concentration as that in the NMR experiment, a major difference was washing, and likely we washed away all of the weakly adsorbed DNA. To test this hypothesis, we then designed a fluorescence experiment without washing (Figure 2C,D). In this case, the fluorescence of 30 nM FAM-MN4 in buffer (5 mM PB with 1 mM $MgCl_2$) was monitored for 3 min. After adding AuNPs, a decrease in fluorescence was observed, which was attributed to DNA adsorption. At 12 min, the fluorescence decreased to 23% of the initial value, suggesting that ~77% of FAM-MN4 was adsorbed. At this point, a final of 200 μM MN4 was added and an obvious increase in the fluorescence was observed, suggesting the displacement of a fraction of the adsorbed FAM-MN4 from the AuNPs. Based on the fluorescence enhancement at 40 min, 14% of the adsorbed FAM-MN4 desorbed. The remaining DNA, however, was still stably adsorbed on the AuNPs despite the presence of the 4000-fold excess of nonlabeled DNA. Combining the washed and unwashed experiments, we concluded that the washed samples washed away the loosely adsorbed MN4 aptamers. Without washing, a fraction of the loosely adsorbed aptamers can be displaced, whereas the remaining tightly adsorbed ones still cannot be desorbed. This experiment can explain the difference between the fluorescence and NMR spectroscopic data. In NMR, AuNPs were directly mixed with concentrated NM4, and it was likely that no stable aptamer adsorption could occur before being displaced by other aptamers. The displacement continued to happen and the adsorbed aptamers had no chance to adopt more stable adsorption conformations. In our fluorescence experiment, for the unwashed system, we initially still added a low concentration of probe DNA, and thus, they had a chance to

https://doi.org/10.1021/acs.langmuir.1c02239
Langmuir 2021, 37, 11939−11947

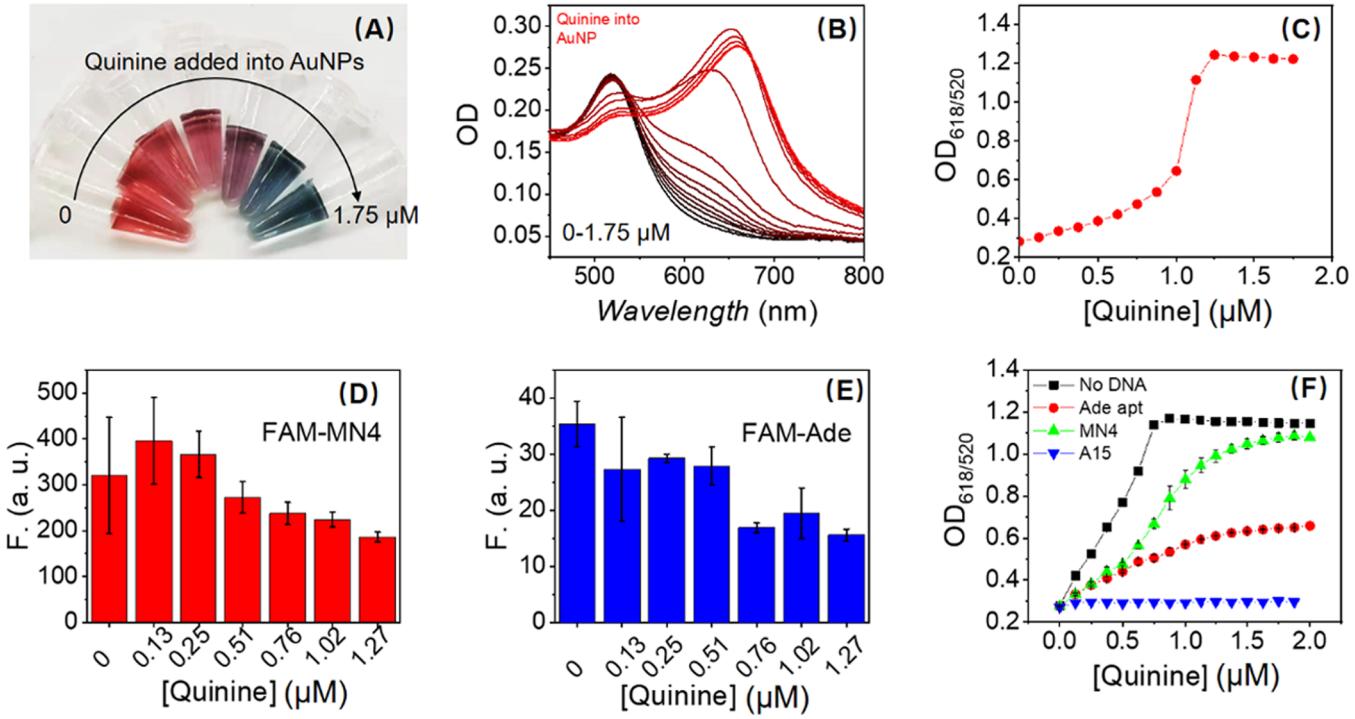

Figure 3. (A) Photograph depicting the color change of AuNPs (5 nM) in the presence of quinine in the range of 0−1.75 μM. Quinine was titrated into 2 nM AuNPs and (B) the UV−vis spectral change, and (C) the extinction ratio as a function of quinine concentration. The adsorption of (D) FAM-MN4 and (E) FAM-Ade aptamer onto AuNPs preadsorbed with different concentrations of quinine. AuNPs (0.5 nM) and 30 nM FAM-MN4 were used and the adsorption buffer contained 5 mM PB and 1 mM $MgCl_2$. (F) The extinction ratio as a function of quinine concentration when quinine was added into 2 nM AuNPs premixed with various DNA in 5 mM PB (pH 7.6).

collapse on the AuNPs to be stably adsorbed. Nevertheless, 14% of the adsorbed aptamers were loosely adsorbed. Without washing, they were displaced by the concentrated nonlabeled aptamers.

As a control, FAM-Ade was tested in the same way. FAM-Ade was added to the AuNPs, and in this case, the quenching was ~38%. After adding 200 μM nonlabeled Ade aptamer, however, almost no fluorescence increase was observed (Figure 2D). We reasoned that the adenosine aptamer was adsorbed more tightly than MN4. MN4 has 6 base pairs in stem 1 to close its structure, whereas the adenosine aptamer has only 4 base pairs, making it more likely to be adsorbed in a collapsed conformation. Each aptamer might be adsorbed differently on AuNPs, but in general, they were all adsorbed very strongly. Thus, aptamer adsorption is under a kinetic control. The dynamics of the aptamer on the AuNPs is related to the initial aptamer concentration, DNA sequence, time of incubation, and washing.

Based on the above results, we depicted the adsorption of MN4, as shown in Figure 2E. At low MN4 concentrations, ~86% of the aptamer was adsorbed strongly (cannot be displaced) and likely in a collapsed state with its secondary structure disrupted. The remaining 14% of the aptamer adsorbed weakly (e.g., in the folded state or adsorbed via interactions with the tightly adsorbed DNA), which can be exchanged with the aptamers in solution. Since the adsorption energy of DNA bases on the gold surface (e.g., via strong coordination interactions) is much stronger than that of DNA base-pairing interactions,[48] thermodynamically, the most stable state for this system is to maximize the contacts between DNA and AuNPs by disrupting internal DNA structures. In the NMR condition, each DNA was well folded and the DNA molecules were so concentrated before mixing with the AuNPs. Therefore, before each adsorbed aptamer had the time to collapse on the AuNPs, exchange with the free aptamers already occurred. NMR showed that adsorption occurred via the tri-adenine loop in stem 2.[28] Since displacement reactions on the gold surface were previously observed with 5-mer DNA homopolymers,[15] it is not surprising to see MN4 displacement with the three confined adenine being the points of adsorption.

Adsorption of Quinine by AuNPs. The above experiments studied free aptamers without adding target molecules. Herein, we introduced the target molecule, quinine. We recently showed that many aptamer target molecules can adsorb on AuNPs and affect the adsorption of their aptamers.[36−41,49] Quinine is a weak base with its first pK_a at 8.5,[50] making it positively charged at neutral pH. In the presence of quinine, AuNPs were aggregated to show blue color (Figure 3A), suggesting quinine adsorption. We then gradually added quinine to the AuNPs and monitored the color change using UV−vis spectroscopy (Figure 3B). The free 13 nm AuNPs had a strong peak at 520 nm, which dropped in intensity upon adding quinine, and a new peak at 618 nm emerged, indicating aggregation of the AuNPs. We then plotted the change of the extinction ratio at 618 nm over that at 520 nm as a function of quinine concentration (Figure 3C), and an apparent K_d of 1.0 μM quinine was obtained. This value was even lower than those measured for dopamine (5.8 μM)[36] and adenosine (7.7 μM),[37] but higher than that for kanamycin (~0.1 μM).[38] Since the AuNP concentration was 2 nM, the number of quinine molecules and the surface sites on the AuNPs was comparable (e.g., each AuNP can accommodate at least 100 quinine based on the capacity for DNA adsorption).

https://doi.org/10.1021/acs.langmuir.1c02239
Langmuir 2021, 37, 11939−11947

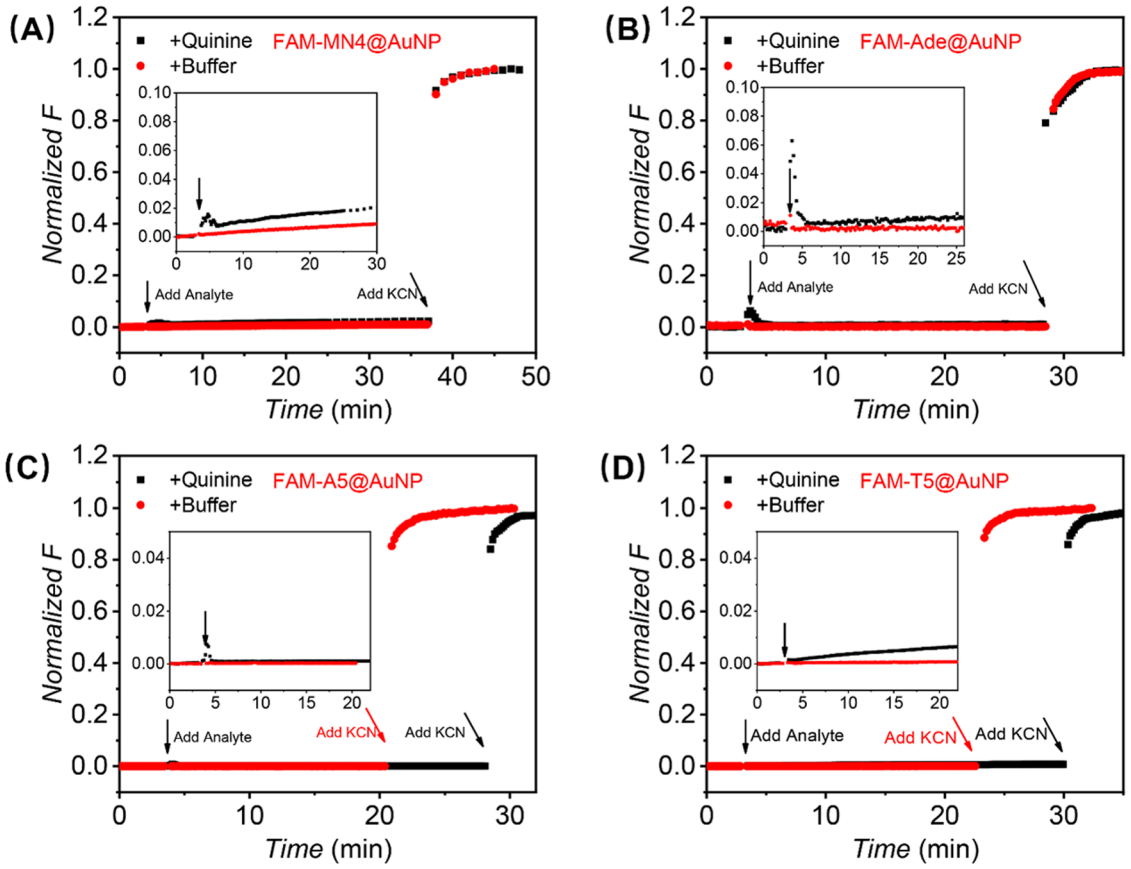

Figure 4. Kinetics of quinine-induced desorption of (A) FAM-MN4; (B) FAM-Ade aptamer; (C) FAM-A_5; or (D) FAM-T_5 from the AuNPs. AuNPs (0.7 nM) were used in (A, B), and 0.5 nM AuNPs were used in (C, D) dispersed in 10 mM PB and 0.8 mM $MgCl_2$. Quinine (100 μM) was added at the time pointed by the arrowheads. In the end, KCN was added to fully desorb the DNA. Insets: the same plot with a smaller *y*-axis scale.

Given the low concentration of quinine needed, the effect of quinine on the aggregation of the AuNPs must be due to its adsorption instead of charge screening as a salt. Given its positive charge, it is not surprising that quinine was potent in aggregating the AuNPs. Therefore, quinine/AuNP interactions need to be considered in this system.

We then studied the effect of quinine on the adsorption of FAM-MN4. We preincubated the AuNPs with various concentrations of quinine and then added FAM-MN4. After incubation and washing, we dissolved the AuNPs using KCN and measured the fluorescence intensity, which represented the adsorbed FAM-MN4 aptamer (Figure 3D). For comparison, we also measured the effect of quinine on the adsorption of the FAM-Ade aptamer (Figure 3E). In both aptamers, the more quinine added, the fewer probes adsorbed. With 1.27 μM quinine, the fluorescence intensity decreased to almost half of the initial value. These two simple experiments demonstrated that quinine can adsorb to the AuNPs and can also inhibit the adsorption of its aptamer or other DNA molecules.

In the NMR experiment, it was observed that adding cocaine inhibited the exchange between the adsorbed and free MN4, and it was attributed to that forming the aptamer/cocaine complex favored the desorbed state. Here, based on our data, it was also possible that a fraction of cocaine or quinine might be adsorbed on the AuNPs to inhibit aptamer adsorption. Since the MN4 aptamer is well folded regardless of binding to target or not, and if adsorption occurred via the tri-adenine loop, the effect of target binding might be small since the loop does not directly participate in target binding. Therefore, we were more inclined to the second mechanism, where target molecule adsorption inhibited the aptamer adsorption and thus the exchange reaction.

After understanding the adsorption of quinine on the AuNPs, we premixed DNA with AuNPs for 20 min and then titrated with quinine to check the aggregation of the AuNPs. Three DNA samples including MN4, adenosine aptamer, and A_{15} were studied. As shown in Figure 3F, the A_{15} sample fully protected the AuNPs, and no aggregation was observed, indicating that the interaction between AuNP and quinine was not strong enough to displace the adsorbed A_{15}. In the presence of the adenosine aptamer, the AuNPs aggregated slightly with a maximum extinction ratio of 0.66. Finally, for MN4, a much higher extinction ratio was reached, indicating more aggregation, although a moderate protection effect still occurred compared to the bare AuNPs. This experiment also indicated that the adsorption of the adenosine aptamer was stronger than the adsorption of MN4, consistent with the abovementioned fluorescent displacement experiment. Overall, the MN4 aptamer only had a weak ability to protect the AuNPs against aggregation caused by quinine.

Feasibility for Fluorescent Sensing. Given that quinine could adsorb to AuNPs, we then tested whether the AuNPs with adsorbed FAM-MN4 can be used as a fluorescent sensor (e.g., via target-induced aptamer desorption). However, even with ~100 μM quinine, the fluorescence only increased by 2% after 25 min (Figure 4A). A similar change was also observed when quinine was added to FAM-Ade/AuNPs (Figure 4B), indicating that the desorption was nonspecific, as the

https://doi.org/10.1021/acs.langmuir.1c02239
Langmuir 2021, 37, 11939−11947

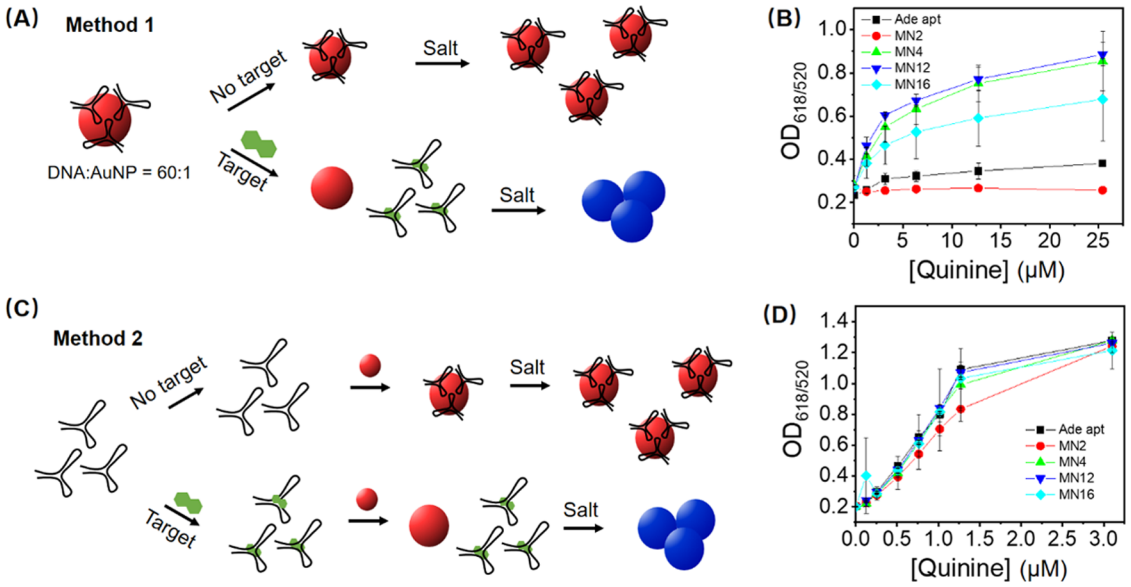

Figure 5. Two methods for label-free quinine colorimetric sensing with AuNPs. (A) The procedure as described in the NMR paper and the expected results. (B) Extinction ratio of 618 and 520 nm as a function of quinine concentration using the method in (A) with five different DNA sequences. (C) The other method where quinine and the aptamer were mixed before adding AuNPs. (D) Extinction ratio following the procedure described in (C) but without adding salt since aggregation of the AuNPs already occurred without additional salt.

adenosine aptamer cannot bind to quinine. From this, we concluded that this system cannot be used as a fluorescent sensor for detecting quinine. This was attributed to the very strong adsorption of the aptamer (note that the sample was washed to achieve a low background fluorescence).

To decrease DNA adsorption affinity, we then used two FAM-labeled 5-mer DNA: A_5 and T_5. We added quinine and monitored the fluorescence change (Figure 4C,D). A small and steady increase was observed in the FAM-T_5 sample, although the desorbed DNA was less than 1%. In addition, no change was seen in the FAM-A_5 sample. This can be explained by the fact that A_5 had a stronger affinity to the AuNPs.[15] Therefore, quinine cannot even desorb T_5 DNA, which is among the weakest affinity oligonucleotide to AuNPs. From these data, although quinine can adsorb on the AuNPs, it cannot desorb the preadsorbed aptamer or DNA. The implication is that when the MN4 aptamer was stably adsorbed under a typical sensing condition, no specific binding of quinine to the adsorbed aptamers can take place. Even if binding occurred, it would not induce aptamer desorption.

Evaluation of the Label-Free Colorimetric Detection Method. Finally, we tested whether quinine can be detected using the classic label-free colorimetric sensing method, which is strongly related to the adsorption of the MN4 aptamer and quinine on AuNPs. Various strategies have been used to detect cocaine using this method. In addition to using the full-length MN4 aptamer,[28] the aptamer was also split into two halves to achieve the detection of cocaine.[26] However, quinine has not been used as a target yet. First, we used the procedure as described in the NMR paper (Figure 5A), where the MN4 aptamer was mixed with 13 nm AuNPs (60:1) followed by adding $MgCl_2$ to assist aptamer adsorption. Without washing, the as-prepared MN4/AuNP mixture was used for quinine sensing. As shown in Figure 5B (the green trace), the MN4 aptamer sample showed increased extinction ratios with higher quinine concentrations, indicating aggregation of the AuNPs. This was consistent with the mechanism described in Figure 5A. However, when we tested two nonbinding mutated aptamers, MN12 and MN16, they also showed an increased extinction ratio. Especially for MN12, its response was identical to that of MN4. We attributed this result to the similar structure of MN12 and MN16 to MN4. MN12 and MN16 only differed by one base compared to the MN4 sequence (Figure 1A), but they had a much weaker binding affinity toward cocaine or quinine. On the other hand, the ATP aptamer and the MN2 mutant showed much less color change. A few base pairs close to the tri-adenine loop were deleted in MN2, which may explain its different behavior compared to MN4. Accordingly, this colorimetric result appeared to be more specific toward the DNA structure rather than binding affinity to targets.

After this, we studied another commonly used sensing procedure (Figure 5C). We first mixed MN4 (300 nM in 100 μL) with different concentrations of quinine in PB (20 mM, pH 7.6) for 15 min and then added AuNPs for colorimetric sensing. After 2 min, the color of the AuNPs already changed to blue. We recorded the extinction ratio and tested the other four DNA mutants and the adenosine aptamer. As shown in Figure 5D, all these DNA exhibited a similar response toward the increase of quinine concentration. The responses were saturated with just 3 μM quinine. We speculated that the aggregation of AuNPs in this experiment was caused by the excess of quinine, which was shown to not only destabilize the AuNPs but also inhibit further DNA adsorption. Overall, the sensing mechanisms shown in Figure 5A,C could not reflect aptamer binding, and neither considered the adsorption of quinine.

Quinine can destabilize the AuNPs, but with the protection of DNA, its destabilization effect decreased. In the presence of quinine, three things can happen. First, fewer DNA could be adsorbed due to the formation of the DNA/quinine complex. Second, quinine could adsorb to destabilize the AuNPs. Third, the adsorbed quinine further inhibited DNA adsorption. All these effects point to the decreased colloidal stability of the AuNPs. Since a similar colorimetric response was observed with the inactive mutants, and quinine cannot induce much

https://doi.org/10.1021/acs.langmuir.1c02239
Langmuir 2021, 37, 11939−11947

aptamer desorption, we do not believe that this colorimetric method can be used for the detection of quinine or for the evaluation of quinine binding by the aptamer. In this experiment, the aptamer was already in a prefolded state, and the effect of quinine binding on the adsorption of the aptamer could be small. To better modulate analyte-dependent aptamer binding, more sophisticated designs such as split aptamers might be required.[26] Even for such engineered aptamers, the test of nonbinding mutants would also be important to confirm the sensing mechanism.

CONCLUSIONS

In this work, we carefully studied the adsorption of the cocaine or quinine aptamer to AuNPs and compared our results with that from a previous NMR work. Our fluorescence work was performed with a much lower concentration of DNA, leading to tighter adsorption. When AuNPs were mixed with a highly concentrated MN4 sample under the NMR condition, the well-folded aptamer could only transiently interact with the AuNPs. Before stable adsorption can be achieved, displacement already took place. Under dilute conditions, the adsorbed MN4 had the time to collapse on the AuNPs and approach a thermodynamically most stable state. We observed the displacement of a small fraction of DNA without washing only for the MN4 aptamer, whereas for the adenosine aptamer, we could not find evidence for its displacement by nonlabeled aptamers even without washing. Therefore, the sequence of DNA, its concentration, incubation time, and washing are all important to determine the outcome of aptamer/AuNP systems. In the second part of this work, the potential of developing fluorescent and colorimetric sensors using the MN4 aptamer was studied. Since quinine cannot induce desorption of the aptamer, a direct dequenching-based fluorescent sensor is difficult to develop. In addition, label-free colorimetric detection was deemed impossible as well for the full-length MN4 aptamer since a similar response was observed with the nonbinding mutants. This can be explained by the strong affinity between quinine and AuNPs, and such target/AuNP interactions were often ignored in most previous works.

AUTHOR INFORMATION

Corresponding Author

Juewen Liu − *Department of Chemistry, Waterloo Institute for Nanotechnology, University of Waterloo, Waterloo N2L 3G1 Ontario, Canada;* orcid.org/0000-0001-5918-9336; Email: liujw@uwaterloo.ca

Author

Fang Zhang − *College of Biological Science and Engineering, Fuzhou University, Fuzhou 350108, People's Republic of China; Department of Chemistry, Waterloo Institute for Nanotechnology, University of Waterloo, Waterloo N2L 3G1 Ontario, Canada*

Complete contact information is available at: https://pubs.acs.org/10.1021/acs.langmuir.1c02239

Notes

The authors declare no competing financial interest.

ACKNOWLEDGMENTS

Funding of the work was from the Natural Sciences and Engineering Research Council of Canada (NSERC) and the National Natural Science Foundation of China (32172285). F.Z. was supported by a China Scholarship Council (CSC) Scholarship to visit the University of Waterloo.

REFERENCES

(1) Elghanian, R.; Storhoff, J. J.; Mucic, R. C.; Letsinger, R. L.; Mirkin, C. A. Selective Colorimetric Detection of Polynucleotides Based on the Distance-Dependent Optical Properties of Gold Nanoparticles. *Science* **1997**, *277*, 1078−1080.

(2) Tan, L. H.; Xing, H.; Lu, Y. DNA as a Powerful Tool for Morphology Control, Spatial Positioning, and Dynamic Assembly of Nanoparticles. *Acc. Chem. Res.* **2014**, *47*, 1881−1890.

(3) Ye, D. K.; Zuo, X. L.; Fan, C. H. DNA Nanostructure-Based Engineering of the Biosensing Interface for Biomolecular Detection. *Prog. Chem.* **2017**, *29*, 36−46.

(4) Cecconello, A.; Besteiro, L. V.; Govorov, A. O.; Willner, I. Chiroplasmonic DNA-Based Nanostructures. *Nat. Rev. Mater.* **2017**, *2*, No. 17039.

(5) Liu, B.; Liu, J. Interface Driven Hybrid Materials Based on DNA-Functionalized Gold Nanoparticles. *Matter* **2019**, *1*, 825−847.

(6) Zhao, W.; Brook, M. A.; Li, Y. Design of Gold Nanoparticle-Based Colorimetric Biosensing Assays. *ChemBioChem* **2008**, *9*, 2363−2371.

(7) Li, L. L.; Xing, H.; Zhang, J. J.; Lu, Y. Functional DNA Molecules Enable Selective and Stimuli-Responsive Nanoparticles for Biomedical Applications. *Acc. Chem. Res.* **2019**, *52*, 2415−2426.

(8) Moon, W. J.; Liu, J. Interfacing Catalytic DNA with Nanomaterials. *Adv. Mater. Interfaces* **2020**, *7*, No. 2001017.

(9) Xue, C.; Xue, Y.; Dai, L.; Urbas, A.; Li, Q. Size- and Shape-Dependent Fluorescence Quenching of Gold Nanoparticles on Perylene Dye. *Adv. Opt. Mater.* **2013**, *1*, 581−587.

(10) Saha, K.; Agasti, S. S.; Kim, C.; Li, X.; Rotello, V. M. Gold Nanoparticles in Chemical and Biological Sensing. *Chem. Rev.* **2012**, *112*, 2739−2779.

(11) Liu, J. Adsorption of DNA onto Gold Nanoparticles and Graphene Oxide: Surface Science and Applications. *Phys. Chem. Chem. Phys.* **2012**, *14*, 10485−10496.

(12) Carnerero, J. M.; Jimenez-Ruiz, A.; Castillo, P. M.; Prado-Gotor, R. Covalent and Non-Covalent DNA−Gold-Nanoparticle Interactions: New Avenues of Research. *ChemPhysChem* **2017**, *18*, 17−33.

(13) Zhang, F.; Wang, S.; Liu, J. Gold Nanoparticles Adsorb DNA and Aptamer Probes Too Strongly and a Comparison with Graphene Oxide for Biosensing. *Anal. Chem.* **2019**, *91*, 14743−14750.

(14) Herne, T. M.; Tarlov, M. J. Characterization of DNA Probes Immobilized on Gold Surfaces. *J. Am. Chem. Soc.* **1997**, *119*, 8916−8920.

(15) Kimura-Suda, H.; Petrovykh, D. Y.; Tarlov, M. J.; Whitman, L. J. Base-Dependent Competitive Adsorption of Single-Stranded DNA on Gold. *J. Am. Chem. Soc.* **2003**, *125*, 9014−9015.

(16) Alkhamis, O.; Canoura, J.; Yu, H. X.; Liu, Y. Z.; Xiao, Y. Innovative Engineering and Sensing Strategies for Aptamer-Based Small-Molecule Detection. *TrAC Trends Anal. Chem.* **2019**, *121*, No. 115699.

(17) Pfeiffer, F.; Mayer, G. Selection and Biosensor Application of Aptamers for Small Molecules. *Front. Chem.* **2016**, *4*, No. 25.

(18) Stojanovic, M. N.; de Prada, P.; Landry, D. W. Fluorescent Sensors Based on Aptamer Self-Assembly. *J. Am. Chem. Soc.* **2000**, *122*, 11547−11548.

(19) Neves, M. A. D.; Shoara, A. A.; Reinstein, O.; Abbasi Borhani, O.; Martin, T. R.; Johnson, P. E. Optimizing Stem Length to Improve Ligand Selectivity in a Structure-Switching Cocaine-Binding Aptamer. *ACS Sensors* **2017**, *2*, 1539−1545.

(20) Neves, M. A. D.; Slavkovic, S.; Churcher, Z. R.; Johnson, P. E. Salt-Mediated Two-Site Ligand Binding by the Cocaine-Binding Aptamer. *Nucleic Acids Res.* **2016**, No. gkw1294.
(21) Yu, H.; Canoura, J.; Guntupalli, B.; Lou, X.; Xiao, Y. A Cooperative-binding Split Aptamer Assay for Rapid, Specific and Ultra-Sensitive Fluorescence Detection of Cocaine in Saliva. *Chem. Sci.* **2017**, *8*, 131−141.
(22) Debiais, M.; Lelievre, A.; Smietana, M.; Müller, S. Splitting Aptamers and Nucleic Acid Enzymes for the Development of Advanced Biosensors. *Nucleic Acids Res.* **2020**, *48*, 3400−3422.
(23) Morris, F. D.; Peterson, E. M.; Heemstra, J. M.; Harris, J. M. Single-Molecule Kinetic Investigation of Cocaine-Dependent Split-Aptamer Assembly. *Anal. Chem.* **2018**, *90*, 12964−12970.
(24) Poltorak, L.; Eggink, I.; Hoitink, M.; Sudholter, E. J. R.; de Puit, M. Electrified Soft Interface as a Selective Sensor for Cocaine Detection in Street Samples. *Anal. Chem.* **2018**, *90*, 7428−7433.
(25) Oueslati, R.; Cheng, C.; Wu, J.; Chen, J. G. Highly Sensitive and Specific on-Site Detection of Serum Cocaine by a Low Cost Aptasensor. *Biosens. Bioelectron.* **2018**, *108*, 103−108.
(26) Zhang, J.; Wang, L. H.; Pan, D.; Song, S. P.; Boey, F. Y. C.; Zhang, H.; Fan, C. H. Visual Cocaine Detection with Gold Nanoparticles and Rationally Engineered Aptamer Structures. *Small* **2008**, *4*, 1196−1200.
(27) Liu, J.; Lu, Y. Fast Colorimetric Sensing of Adenosine and Cocaine Based on a General Sensor Design Involving Aptamers and Nanoparticles. *Angew. Chem., Int. Ed.* **2006**, *45*, 90−94.
(28) Mirau, P. A.; Smith, J. E.; Chávez, J. L.; Hagen, J. A.; Kelley-Loughnane, N.; Naik, R. Structured DNA Aptamer Interactions with Gold Nanoparticles. *Langmuir* **2018**, *34*, 2139−2146.
(29) Shi, X. X.; Xu, H.; Wu, Y. N.; Zhao, Y. M.; Meng, H. M.; Li, Z. H.; Qu, L. B. Two-Dimension (2D) Cu-MOFs/Aptamer Nanoprobe for in Situ ATP Imaging in Living Cells. *J. Anal. Test.* **2021**, *5*, 165−173.
(30) Tao, X. Q.; Liao, Z. Y.; Zhang, Y. Q.; Fu, F.; Hao, M. Q.; Song, Y.; Song, E. Q. Aptamer-Quantum Dots and Teicoplanin-Gold Nanoparticles Constructed Fret Sensor for Sensitive Detection of Staphylococcus Aureus. *Chin. Chem. Lett.* **2021**, *32*, 791−795.
(31) Wang, L.; Zhang, H.; Wang, C.; Xu, Y.; Su, J.; Wang, X.; Liu, X.; Feng, D.; Wang, L.; Zuo, X.; Shi, J.; Ge, Z.; Fan, C.; Mi, X. Poly-Adenine-Mediated Spherical Nucleic Acids for Strand Displacement-Based DNA/RNA Detection. *Biosens. Bioelectron.* **2019**, *127*, 85−91.
(32) Zhang, X.; Liu, B.; Dave, N.; Servos, M. R.; Liu, J. Instantaneous Attachment of an Ultrahigh Density of Nonthiolated DNA to Gold Nanoparticles and Its Applications. *Langmuir* **2012**, *28*, 17053−17060.
(33) Pei, R.; Shen, A.; Olah, M. J.; Stefanovic, D.; Worgall, T.; Stojanovic, M. N. High-Resolution Cross-Reactive Array for Alkaloids. *Chem. Commun.* **2009**, No. 3193.
(34) Reinstein, O.; Yoo, M.; Han, C.; Palmo, T.; Beckham, S. A.; Wilce, M. C. J.; Johnson, P. E. Quinine Binding by the Cocaine-Binding Aptamer. Thermodynamic and Hydrodynamic Analysis of High-Affinity Binding of an Off-Target Ligand. *Biochemistry* **2013**, *52*, 8652−8662.
(35) Smith, J. E.; Griffin, D. K.; Leny, J. K.; Hagen, J. A.; Chávez, J. L.; Kelley-Loughnane, N. Colorimetric Detection with Aptamer-Gold Nanoparticle Conjugates Coupled to an Android-Based Color Analysis Application for Use in the Field. *Talanta* **2014**, *121*, 247−255.
(36) Liu, X.; He, F.; Zhang, F.; Zhang, Z.; Huang, Z.; Liu, J. Dopamine and Melamine Binding to Gold Nanoparticles Dominates Their Aptamer-Based Label-Free Colorimetric Sensing. *Anal. Chem.* **2020**, *92*, 9370−9378.
(37) Zhang, F.; Huang, P.-J. J.; Liu, J. Sensing Adenosine and ATP by Aptamers and Gold Nanoparticles: Opposite Trends of Color Change from Domination of Target Adsorption Instead of Aptamer Binding. *ACS Sensors* **2020**, *5*, 2885−2893.
(38) Zhou, J.; Li, Y.; Wang, W.; Lu, Z.; Han, H.; Liu, J. Kanamycin Adsorption on Gold Nanoparticles Dominates Its Label-Free Colorimetric Sensing with Its Aptamer. *Langmuir* **2020**, *36*, 11490−11498.
(39) Zong, C.; Liu, J. The Arsenic-Binding Aptamer Cannot Bind Arsenic: Critical Evaluation of Aptamer Selection and Binding. *Anal. Chem.* **2019**, *91*, 10887−10893.
(40) Zong, C.; Zhang, Z.; Liu, B.; Liu, J. Adsorption of Arsenite on Gold Nanoparticles Studied with DNA Oligonucleotide Probes. *Langmuir* **2019**, *35*, 7304−7311.
(41) Hu, Y.; Huang, Z.; Liu, B.; Liu, J. Hg(II) Adsorption on Gold Nanoparticles Dominates DNA-Based Label-Free Colorimetric Sensing. *ACS Appl. Nano Mater.* **2021**, *4*, 1377−1384.
(42) Zhang, F.; Liu, J. Label-Free Colorimetric Biosensors Based on Aptamers and Gold Nanoparticles: A Critical Review. *Anal. Sens.* **2021**, *1*, 30−43.
(43) Liu, J.; Lu, Y. Preparation of Aptamer-Linked Gold Nanoparticle Purple Aggregates for Colorimetric Sensing of Analytes. *Nat. Protoc.* **2006**, *1*, 246−252.
(44) Neves, M. A. D.; Reinstein, O.; Johnson, P. E. Defining a Stem Length-Dependent Binding Mechanism for the Cocaine-Binding Aptamer. A Combined Nmr and Calorimetry Study. *Biochemistry* **2010**, *49*, 8478−8487.
(45) Petrovykh, D. Y.; Perez-Dieste, V.; Opdahl, A.; Kimura-Suda, H.; Sullivan, J. M.; Tarlov, M. J.; Himpsel, F. J.; Whitman, L. J. Nucleobase Orientation and Ordering in Films of Single-Stranded DNA on Gold. *J. Am. Chem. Soc.* **2006**, *128*, 2−3.
(46) Storhoff, J. J.; Elghanian, R.; Mirkin, C. A.; Letsinger, R. L. Sequence-Dependent Stability of DNA-Modified Gold Nanoparticles. *Langmuir* **2002**, *18*, 6666−6670.
(47) Liu, B.; Wu, P.; Huang, Z.; Ma, L.; Liu, J. Bromide as a Robust Backfiller on Gold for Precise Control of DNA Conformation and High Stability of Spherical Nucleic Acids. *J. Am. Chem. Soc.* **2018**, *140*, 4499−4502.
(48) Östblom, M.; Liedberg, B.; Demers, L. M.; Mirkin, C. A. On the Structure and Desorption Dynamics of DNA Bases Adsorbed on Gold: A Temperature-Programmed Study. *J. Phys. Chem. B* **2005**, *109*, 15150−15160.
(49) Tao, X.; He, F.; Liu, X.; Zhang, F.; Wang, X.; Peng, Y.; Liu, J. Detection of Chloramphenicol with Aptamer-Based Colorimetric Assay: Critical Evaluation of Specific and Unspecific Binding of Analyte Molecules. *Microchimica Acta* **2020**, *187*, No. 668.
(50) Strauch, S.; Dressman, J. B.; Shah, V. P.; Kopp, S.; Polli, J. E.; Barends, D. M. Biowaiver Monographs for Immediate-Release Solid Oral Dosage Forms: Quinine Sulfate. *J. Pharm. Sci. A* **2012**, *101*, 499−508.

https://doi.org/10.1021/acs.langmuir.1c02239
Langmuir 2021, 37, 11939−11947